FROM THE INSTITUTE OF RADIOPHYSICS (DIRECTOR: PROF. R. SIEVERT), KAROLINSKA SJUKHUSET, STOCKHOLM, SWEDEN.

EXIT DOSE MEASUREMENTS IN COBALT 60 TELETHERAPY

by

LENNART SUNDBOM

A suitable irradiation technique in radiotherapy is generally worked out with the aid of standard isodose charts, established from dose measurements in a large homogeneous phantom. The International Commission on Radiological Units and Measurements (ICRU 1963) has recommended that the measurements be made in a cubic water phantom with sides of at least 30 cm. The beam is usually directed at right angles to the plane surface of the phantom. When there are differences of radiophysical significance, between these standardized conditions and those arising in the irradiation of a patient, either the charts must be corrected or, in appropriate cases, compensation must be made for the differences. Since both the correction and compensation methods are approximate, some difference may remain between the dose distribution determined and the distribution actually obtained. Errors also occur due to limited accuracy in the determination of geometrical quantities. It therefore seems desirable that the dose in an irradiated volume should be checked by means of measurements during actual treatment. The most advantageous

Submitted for publication 23 June 1964.

solution is naturally to measure the dose at the points where accuracy is important, such as in the tumour volume and in organs of high radiosensitivity. This cannot, however, at present be generally achieved in practice.

Measurements with so-called Bg-chambers have been made at Radiumhemmet for a number of years on the exit side of a patient, in order to estimate the dose along the axis of the beam. This radiation detector has been shown by SIEVERT (1934), SKÖLDBORN (1959) and by DAHL & VIKTERLÖF (see HULTBERG et coll. 1959) to have a low energy dependence and to give good reproducibility. It is the aim of this paper to elucidate the theoretical assumptions for using exit dose measurements to calculate the dose distribution in a patient.

Methods for making individual corrections to standard dose distributions by means of exit dose measurements have been previously described.

KORNELSEN (1954) determined correction factors along the axis of the beam for roentgen irradiation (HVL 1.3 mm Cu) by using a 3 cm diameter ion chamber. He made use of the established relationship: the logarithm of the dose decreases proportionately with the depth (except near the surface), and obtained a satisfactory accuracy when using two beams in opposite positions.

WOODLEY et coll. (1960) measured the exit dose for 250 kV and 2 MV roentgen rays by means of an ion chamber with a collecting electrode of 3 cm diameter. The deflection of the measuring instrument was expressed as a function of the thickness of a water phantom placed in the beam. The equivalent water thickness of the patient was read off on this diagram, and the doses at points within the irradiated tissue volume were corrected proportionally, unless knowledge of anatomical inhomogeneities permitted a discontinuous modification of the internal portion of the treatment plan.

Treatment units and measuring equipment. The measurements described below were carried out with the kilocurie cobalt 60 units at Radiumhemmet: Gammatron I (HULTBERG et coll. 1959) and Eldorado Super G (HULTBERG et coll. 1962). These are equipped with block diaphragms, the first with its front at 31 cm and the other with its front at 35 cm from the source, the source in each case being 2 cm in diameter. A light beam simulating the geometry of the gamma beam is used.

Except where otherwise stated, the measurements were made in a water phantom ($30 \times 30 \times 40$ cm) with perspex walls by using an ion chamber (BENNER et coll. 1959) with an outer diameter of 4.5 mm and a length of 15 mm. This chamber in comparative studies was found to give the same results as Bg-chambers for this type of measurement. The positioning of the chamber in the desired position in the phantom was simplified by using an automatic isodose recorder (LARSSON et coll. 1963). The ionization current was amplified

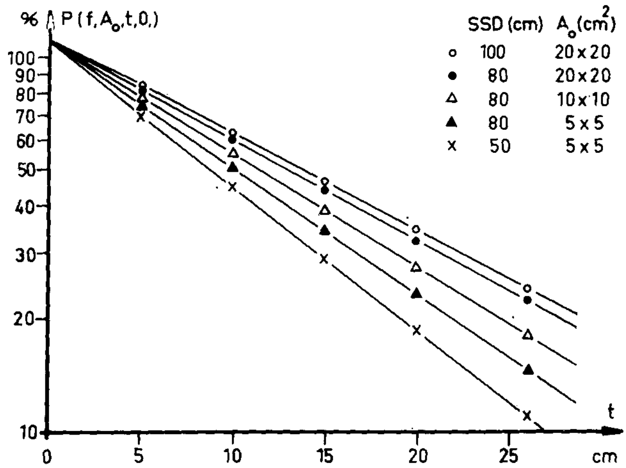

Fig. 1. Logarithm of the percentage dose along the beam axis as a function of the depth. Values taken from Brit. J. Radiol. Suppl. 10.

with a vibrating-reed electrometer. In all the measurements at least 10 cm of water, or mix-D, were located behind the chamber recording the 'exit dose'.

Method of calculation

Derivation of formulas for square beams. A coordinate system has been introduced to make it easier to define the position of a point in the beam. This system has its origin along the beam axis at a distance from the source equal to the source-surface distance. The x and y axes are perpendicular to the beam axis and parallel to the sides of the rectangular beam. The t axis coincides with the beam axis. For symmetric rectangular beams, the cross-section at a depth of 0.5 cm in the phantom is defined as

$$A_0 = 2a \times 2a \tag{1}$$

and is called field size, (a, 0, 0.5) being the coordinate along the x axis for the point where the dose is 50 % of that at the point (0, 0, 0.5), and (0, a, 0.5) being the coordinate along the y axis of the point where the dose is 50 % of that at the point (0, 0, 0.5).

By expressing the dose along the axis of the beam as a function of the depth, with the field size as parameter, we obtain straight lines in a log-linear diagram for depths greater than 5 cm. The dose at depth t, as a percentage of the dose at 0.5 cm, is expressed by

$$P(f, A_0, t, s) \tag{2}$$

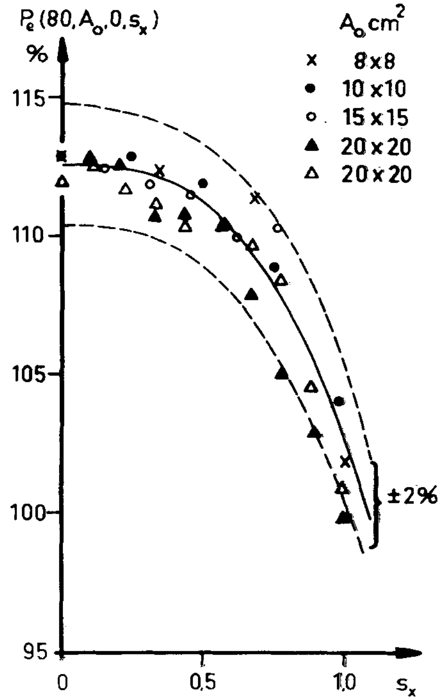

Fig. 2. The extrapolated percentage surface dose as a function of the position in the equivalent standard isodose chart. The continuous line obtained by the method of least squares from the standard isodose charts. The points plotted are calculated from doses measured at depths of 20 and 10 cm.

were f is the source-surface distance,
A_0 is the field size, i.e. the cross-section of the beam, at a depth of 0.5 cm in the phantom,
t is the depth in the phantom, and
s is a function of the distance to the beam axis; this is defined in eq. (5). In this case: $s = 0$.

The values in Fig. 1 have been taken from the British Journal of Radiology, Supplement No. 10 (1961). When the straight lines are extrapolated to the surface they come very close to the same point. The extrapolated value for $t = 0$ varies only by a small percentage for source-surface distances in the range between 50 and 100 cm and for field sizes between 5×5 cm and 20×20 cm. All the cases dealt with below concern the relationships with a nominal SSD of 80 cm and with field sizes between 5×5 cm and 20×20 cm. The extrapolated value, expressed by $P_e(f, A_0, 0, 0)$, was calculated by the method of least squares giving:

$$P_e(80, A_0, 0, 0) = 112.5 \pm 1\% \tag{3}$$

where $25 < A_0 < 400$ cm^2.

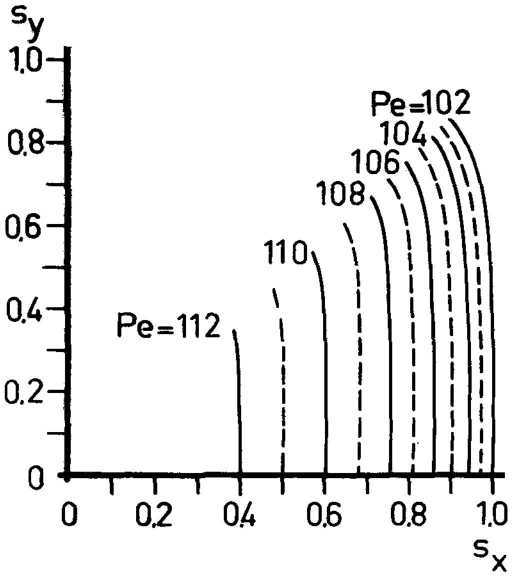

Fig. 3. The extrapolated percentage surface dose as a function of the position in the field. $s_x = \frac{x}{a-1}$ and $s_y = \frac{y}{a-1}$ express the position in the field; x and y are two mutually perpendicular coordinate axes parallel with the sides of the field with their origins at the centre of the field; a and a are the coordinates of the field limits.

Even for lines parallel to the axis of the beam, the logarithm of the dose decreases approximately linearly with the depth in the phantom. Measurements have shown this relationship to hold within the whole useful area of the beam. With 'useful area' we mean the area where the dose is greater than, or equal to, 90 % of the dose in the centre of the beam at a given depth. This approximately applies in an area with a cross-section of $2(a - 1) \times 2(a - 1)$ at all depths in the phantom for the two above mentioned cobalt 60 units.

$P_e(80, A_0, 0, s)$ for lines parallel with the beam axis was calculated by the method of least squares from previously measured two-dimensional standard isodose charts. These charts show the dose distribution in a principal plane, i. e. a plane along the beam axis and parallel with two of the sides of the rectangular field (ICRU 1963). This plane can be the $x - t$ plane. If P_e is expressed as a function of the x coordinate, the curves obtained for the various field sizes are all of the same shape. It was previously shown that the value at the origin is approximately independent of the field size. Since this is the case for $x = a - 1$ too, we define s_x

$$s_x = \frac{x}{a-1} \tag{4}$$

Then all the curves nearly coincide. The curve in Fig. 2 was established on the basis of the values of P_e (80, A_0, 0, s) calculated from the standard isodose charts. The points plotted were obtained by extrapolating to the surface the lines through the dose values measured at the depths of 10 and 20 cm. It will be seen that all the points plotted for the various square fields lie within $\pm$ 2 % of the curve. The measurements for the field size 20 $\times$ 20 cm were made on two different occasions.

The dose measurements at the depths of 10 and 20 cm were extended to the whole planes. The diagram in Fig. 3 was obtained by extrapolation to the surface, giving the relationship between P_e (80, A_0, 0, s) and the intersection point of the line with the surface. This point is defined by the function s which gives the position in the x—y plane of a line parallel to the beam axis

$$s=(s_x; s_y)=\left(\frac{x}{a-1}; \frac{y}{a-1}\right) \tag{5}$$

The percentage dose along a line parallel with the beam axis may thus be expressed as follows for depths t and t_p, respectively:

$$\left.\begin{aligned} P(f, A_0, t, s) &= P_e(f, A_0, 0, s) \cdot e^{m(f, A_0, s) \cdot t} \\ P(f, A_0, t_p, s) &= P_e(f, A_0, 0, s) \cdot e^{m(f, A_0, s) \cdot t_p} \end{aligned}\right\} \tag{6}$$

where m is the angular coefficient for the corresponding straight line in the log-linear diagram (cf. Fig. 1). In the following t_p is used to indicate the thickness of the irradiated object parallel to the beam axis.

By substitution:

$$P(f, A_0, t, s)=[P_e(f, A_0, 0, s)]^{\frac{t_p-t}{t_p}} \cdot [P(f, A_0, t_p, s)]^{\frac{t_p}{t}} \tag{7}$$

The percentage dose at an arbitrarily chosen point (x, y, t) can then be calculated when the percentage dose at a depth t_p is known.

When the 'centre dose' has to be calculated, i. e. the dose midway between the entrance and exit surfaces, eq. (7) may be simplified to

$$P(f, A_0, t_p/2, s)=\sqrt{P_e(f, A_0, 0, s) \cdot P(f, A_0, t_p, s)} \tag{8}$$

Since $P(f, A_0, t_p, s)$ is the dose measured at the exit surface, the thickness of the irradiated object need not be known for these calculations.

For doses along the beam axis, additional simplifications may be made

$$P(f, A_0, t_p/2, 0)=\sqrt{P_e(f, A_0, 0, 0) \cdot P(f, A_0, t_p 0)} \tag{9}$$

By putting $P(f, A_0, t_p/2, 0) = P_C$, which means the centre dose as a percentage of the dose at 0.5 cm,

$P(f, A_0, t_p, O) = P_E$, which means the exit dose as a percentage of the dose at 0.5 cm, and

$\sqrt{P_e(80, A_0, 0, 0)} = \sqrt{112.5} = 10.6$; cf eq. (3),

eq. (9) may be simplified to

$$P_C = 10.6\sqrt{P_E} \tag{10}$$

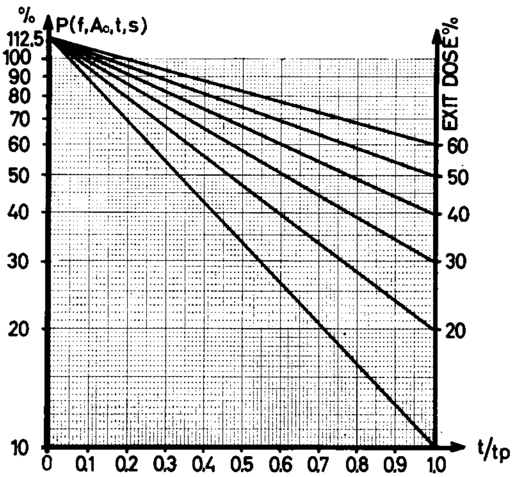

Fig. 4. Diagram for determination of the percentage dose at a given depth (t) from the exit dose (measured at depth t_p). The lines drawn apply to the dose along the beam axis.

The centre dose may then be calculated without knowing the values of A_0 and t_p. Since from the diagram in Fig. 3, $P_e(80, A_0, 0, 0)$ only varies between the values 102 % and 113 %, eq. (10) can be used within the whole of the 'useful area' with a margin of error of $\pm$ 3 % if the constant 10.6 is replaced by 10.4. This equation is often used in pratice.

Eq. (7) may also be solved graphically with the aid of a log-linear diagram. The principle is evident from Fig. 4. The procedure for the determination of a dose at an arbitary depth t, when the exit dose at a depth t_p is known, is as follows: s_x and s_y are determined; P_e is read from the diagram in Fig. 3; a straight line is drawn on a log-linear diagram between P_e and the measured value of the exit dose; $P(f, A_0, t, s)$ is read off for the desired depth.

With the aid of the values in the depth-dose table mentioned, it was found that this method gives an error not exceeding 1 to 2 % along the beam axis up to 4 cm from the surface. The error is greater nearer the surface, at $t = 2$ cm a value approximately 5 % too high is obtained. In practice, however, correction with the aid of exit dose measurements of the standard dose distributions nearer the surface than 4 cm would only be of interest in exceptional cases.

An experimental investigation was performed in order to establish the magnitude of the errors introduced when this calculation method is used in practice.

Verification of the formulas for varying depths. The doses were measured in one of the principal planes at points along L_1 and L_3 in the water phantom accord-

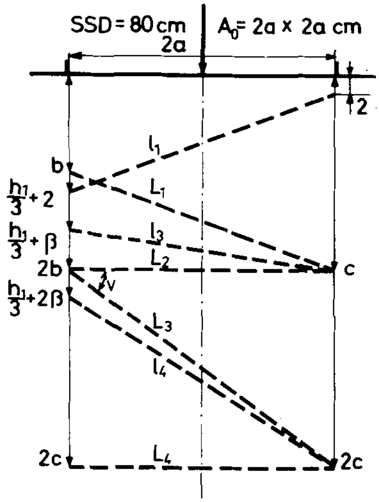

A_0 cm²	b cm	c cm	v°	β cm	h_1 cm
8×8	6	12	56	8	8
15×15	6	12	39	4.5	15
20×20	7.5	15	37	5	20

Fig. 5. Measuring arrangement at a perpendicularly incident beam. Cross section through the water phantom in a principal plane of the beam. Those lines are marked along which the measurements are made.

ing to Fig. 5. The distances of the points perpendicular to the beam axis were 1, 2, 3, . . . cm. The field sizes were 8 $\times$ 8 cm, 15 $\times$ 15 cm and 20 $\times$ 20 cm, respectively; for the first two of the field sizes mentioned the distance (t_p) from the surface to the line L_3 varied from 12 to 24 cm and for the last field size, from 15 to 30 cm. Starting from the values along L_3, the equivalent values along L_1 were calculated with eq. (8). The maximum deviation from the directly measured values was found to be within $\pm$ 3 %.

Verification of the formulas for beams that are not square. The dose was measured over a plane at a depth of 20 cm at 1 cm intervals for field sizes of 5 $\times$ 20 cm and 10 $\times$ 20 cm. The doses at equivalent points at a depth of 10 cm were calculated with eq. (8) and compared with those measured at the same points. The maximum deviation between the corresponding values was $\pm$ 2 %.

It is thus evident that the dose in an irradiated water phantom may be calculated relatively simply by means of the exit dose measured under the same conditions as those existing when the standard isodose charts are obtained. With this established, the applicability of the method for the two conditions under which correction of the standard isodose charts will be necessary (for ^{60}Co γ-radiation) for accurate dose planning may now be discussed. Those conditions occur when the beam strikes a body contour obliquely and when the beam passes through an air-filled lung.

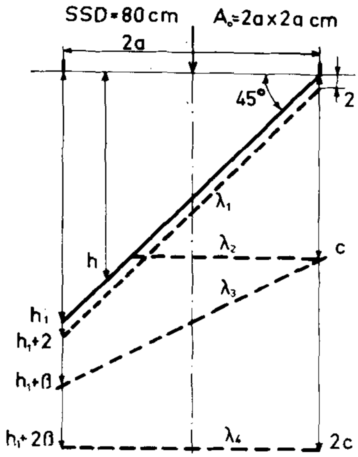

A_0 cm^2	h_1 cm	β cm	c cm
8×8	8	8	12
15×15	15	4.5	12
20×20	20	5	15

Fig. 6. Measuring arrangement at obliquely incident beam. Cross-section through the water phantom in a principal plane of the beam. Those lines are marked along which the measurements are made.

Calculation of dose distribution for obliquely incident beams

Calculation with the aid of exit dose measurements. A correction must be made in eq. (7) for obliquely incident beams. Since the intensity of the beam in air decreases approximately as the square of the distance from the radiation source, this is assumed to apply for $P_e\,(f, A_0, 0, s)$ as well. Thus we obtain

$$P\,(f, A_0, t, s) = \left[\left(\frac{f}{f+h}\right)^2 P_e(f, A_0, 0, s)\right]^{\frac{t_p-t}{t_p}} \cdot [P\,(f, A_0, t_p, s)]^{\frac{t}{t_p}} \qquad (11)$$

where h is the distance between the nominal and the actual surface measured parallel to the beam axis (cf. Fig. 6).

This equation was confirmed experimentally for field sizes of 8 × 8 cm, 15 × 15 cm and 20 × 20 cm, by measurements schematically shown in Fig. 6. The water phantom was placed at 45° to the beam axis; a further water phantom with 4 mm perspex walls was located between the nominal and the actual incident surfaces in order to determine the accuracy of the measurements. The dose was measured along the lines λ_2 and λ_4 and compared with the values at the equivalent points along the lines L_2 and L_4, shown in the experimental set-up in Fig. 5. The maximum deviation was $\pm$ 2 %.

The wedge-shaped phantom was then removed and the dose was measured along the lines λ_1, λ_3 and λ_4 at the distances 1, 2, 3, . . . cm perpendicular to the beam axis. Starting from the values along line λ_4, the values along λ_1 and λ_3 were calculated by solving eq. (11) graphically (cf Fig. 4); 5 % was added to the values along line λ_1, situated at a depth of 2 cm. A comparison with the directly measured values revealed a maximum error of $\pm$ 3 %. Without correction, the maximum deviation from the standard isodose charts is

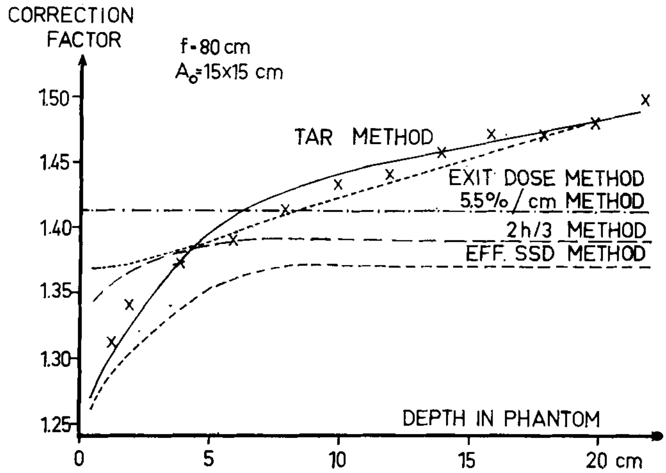

Fig. 7. Comparison between various methods for correcting standard isodose charts for obliquely incident beams. The correction factor, as a function of the depth in a water phantom placed as in fig. 6. The crosses indicate the values measured.

+ 140 %. The values corresponding to these charts were obtained by measuring the dose with the wedge phantom in the beam.

Comparison with other methods of calculation. A method of correcting the standard isodose charts for obliquely incident beams has been described by Du Sault & Legaré (1963). This involves multiplying the dose in the charts by the factor

$$k_r = \frac{T\,(A, t)}{T\,(A,\ t+h)} \tag{12}$$

where A is the beam size at the depth $t + h$ cm,

t is the depth in the phantom along a line from the radiation source to the point considered,

h is the distance between the nominal and the actual surfaces along the same line (in this case *not* parallel with the beam axis), and

$T\,(A,\ t)$ are tissue-air ratios (TAR) in accordance with 'Clinical Dosimetry' (ICRU 1963).

Independent of this investigation, it was observed (Sundbom 1964) that when using compensating filters greater accuracy was achieved by applying TAR for the beam size at a depth of 0.5 cm instead of TAR for the beam size at the actual depth, i. e.

$$k_r = \frac{T\,(A_0, t)}{T\,(A_0, t+h)} \tag{13}$$

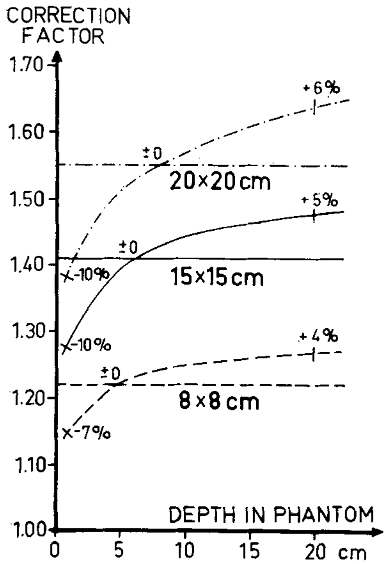

Fig. 8. Comparison between two methods for correcting standard isodose charts for obliquely incident beams. The correction factor, as a function of the depth in a water phantom placed as in fig. 6, with the field size as parameter. The straight lines are obtained by the '5.5 % per centimetre method' and the curved lines by the TAR method. The inserted figures represent the differences between values given by the two methods as a percentage of the TAR method.

The latter method is easier to use because no interpolation for the variation of the beam size with depth is required. Eq. (13) was checked experimentally by measuring the dose along the lines λ_1, λ_3, and λ_4 with the experimental set-up shown in Fig. 6. The values obtained with the wedge phantom in the beam were multiplied by k_r, defined according to eq. (13). All the values measured without the wedge phantom were within $\pm$ 3 % of those calculated for the used field sizes 8 $\times$ 8 cm, 15 $\times$ 15 cm, and 20 $\times$ 20 cm. As was pointed out previously, the maximum deviation from the standard isodose charts is + 140 %.

This method is rather laborious for the correction of charts in manual dose planning. Three other methods have been given in the literature and these might be called: (1) the effective attenuation coefficient method, (2) the effective SSD method, and (3) the isodose curve shift method. These have been described by ICRU (1963) and compared for accuracy by GARRETT & JONES (1962), and by DUTREIX & DUTREIX (1962); references to the original work on the different methods were included.

The effective attenuation coefficient method is from here on replaced by increasing the dose by 5.5 % per cm 'missing tissue' in accordance with JOHNS (1961). Thus h and t are determined as in the exit dose method, i. e. the distances are measured parallel with the beam axis. Using the isodose curve shift method, the curves are displaced parallel with the beam axis $\frac{2}{3}$ h.

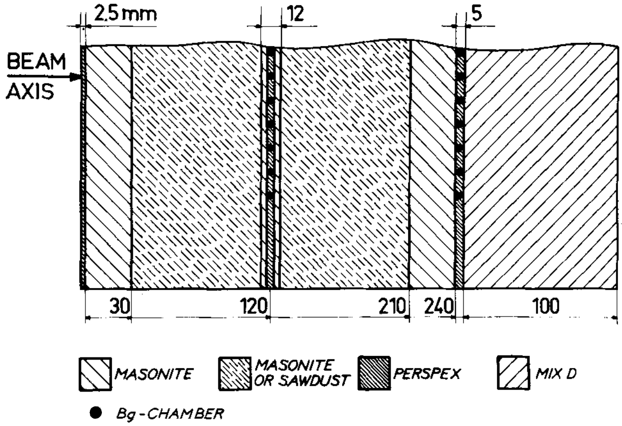

Fig. 9. Cross-section through masonite phantom. The masonite sheets (30 × 30 cm) can be replaced by sawdust (0.25 g/cm³) between 30 mm and 210 mm. The black dots indicate Bg-chambers; these are inserted into perspex sheets. Mix-D is placed behind the phantom.

The correction factor along the axis of the beam obtained by five correction methods is shown in Fig. 7, for a field size of 15 × 15 cm, as a function of the depth in the phantom. The phantom was placed as shown in Fig. 6. When using the exit dose method of correction, t_p (the thickness of the irradiated object) was put equal to 20 cm. Comparison with the measured values indicates that all the methods, except the TAR and the exit dose methods, give too low a correction factor at large depths; this is especially true for the effective SSD method. Near the surface of the phantom, all the methods, except the TAR method and the effective SSD method, give correction factors that are too high. The variation of the correction factors with field size and depth in the phantom is illustrated in Fig. 8 according to the TAR method and the '5.5 % per centimetre method'. The latter method thus gives quite high accuracy in spite of its simplicity.

A comparison between methods (1), (2) and (3) was made at various points within the beam in a series of measurements. This showed the isodose curve shift method to give results quite as accurate as the others. This method has the advantage of being simple to apply to individual irradiation planning. The accuracy was investigated with the aid of dose measurements with the experimental set-up in Figs 5 and 6, for field sizes 8 × 8 cm, 15 × 15 cm and 20 × 20 cm. The lines λ_1, λ_3 and λ_4 were projected in the phantom placed as for measurement of standard isodose charts. This gave the lines l_1, l_3 and l_4 in Fig. 5. A comparison of the doses at equivalent points on equivalent lines revealed the following maximum deviations

for field size	8 × 8 cm	± 2 %
» » »	15 × 15 cm	± 5 %
» » »	20 × 20 cm	± 6 %

with the exception of the points along the line λ_4 (and the corresponding line l_4 in Fig. 5) from the right-hand limit of the field half-way to the beam axis. The maximum deviations for the various field sizes were + 5 %, +12% and + 15 %, respectively. These values should be compared with the maximum deviation of + 140 % that occurs when no correction is made.

Calculation of dose distribution for beam passing through air-filled lung

The exit dose method was found to be applicable even for calculation of the dose in the irradiation of lung tissue. The assumption that this should be the case is based on the investigations carried out by Burlin (1957). This author reported that correction methods, based on absorption differences only, lead to an excessive correction factor, but that corrections based on exit dose measurements produce relatively accurate correction factors. A number of experiments were made to determine the magnitude of the difference between the calculated and the measured doses. These included measurements with Bg-chambers.

The experimental set-up is depicted in Fig. 9. This shows a cross-section of the used masonite phantom (30 × 30 × 24 cm). The Bg-chambers were introduced into sheets of perspex 5 mm thick. A varying number of masonite sheets, at depths between 3 cm and 21 cm, were replaced with sawdust with a density of 0.25 g/cm³. This is the same sawdust that was stated by Dahl & Vikterlöf (1960) to be radiation-equivalent to an air-filled lung. The replacement, 3 cm at a time, was made both from right to left, and vice-versa, as well as from the central perspex sheet and outwards. The field sizes were 7.5 × 7.5 cm and 15 × 15 cm. The measured values of the exit dose were put into eq. (8), giving the doses in the central plane of the phantom. The corresponding values of the dose measured in this plane at the same time varied between 107 % and 90 % of that calculated. The 90 % value (i. e. a dose 10 % too low) was obtained when 9 cm of sawdust was placed in front of the central perspex sheet with only masonite behind the perspex. This result was expected and is due to the 'build-up' of the scattered radiation (Burlin 1957).

The same exposure to two opposed beams (with a varying sawdust-masonite distribution as above) gave a measured dose varying between 102 % and 95 % of that calculated. The 95 % value (i. e. a dose 5 % too low) was obtained when all the masonite was replaced by sawdust.

The equivalent measurements and calculations were made with the same experimental set-up but with the chamber holder moved from the centre of the phantom to depths of 6 and 18 cm, respectively. The same degree of deviation was obtained between the measured and the calculated doses in these cases.

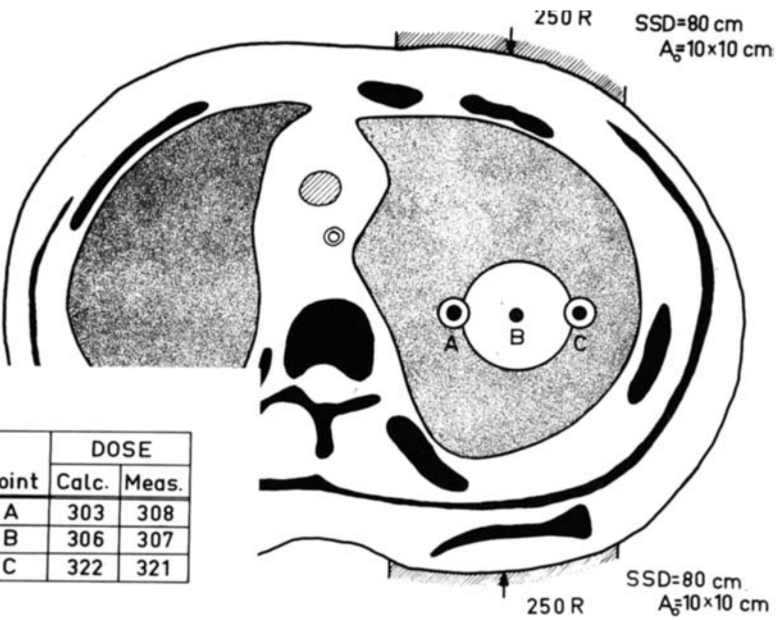

	DOSE	
Point	Calc.	Meas.
A	303	308
B	306	307
C	322	321

Fig. 10. Cross-section through an anatomical thorax phantom containing a mix-D cylinder (5 cm in diameter). The positions of the beams are shown. The doses at points A, B, and C were calculated with the aid of exit dose measurements and measured directly. Dose in rad.

A simple method of correcting for an air-filled lung at the dose planning was tested. This consists in increasing the dose given by a standard isodose chart by 3 % for each centimetre of lung through which the beam passes. The dose was calculated in this way for both the above experiments, both within the phantom and at the exit surface. In no case did the calculated dose deviate more than ± 10 % from the measured dose. This degree of accuracy is obtained if the density of the air-filled lung is 0.25 g/cm³ within the whole beam and if the geometric dimensions are known. The dose was increased to a maximum of 160 % at the exit plane and 140 % in the planes inside the phantom.

Calculation of dose distribution in an anatomical thorax phantom

The method of calculation of the dose distribution with the aid of exit dose measurements was tested by the irradiation of an anatomical thorax phantom. The phantom is formed by a skeleton and mix-D with an air-filled lung represented by sawdust with a density of 0.25 g/cm³ (Dahl & Vikterlöf 1960). A mix-D cylinder with a diameter of 5 cm and with channels for Bg-chambers

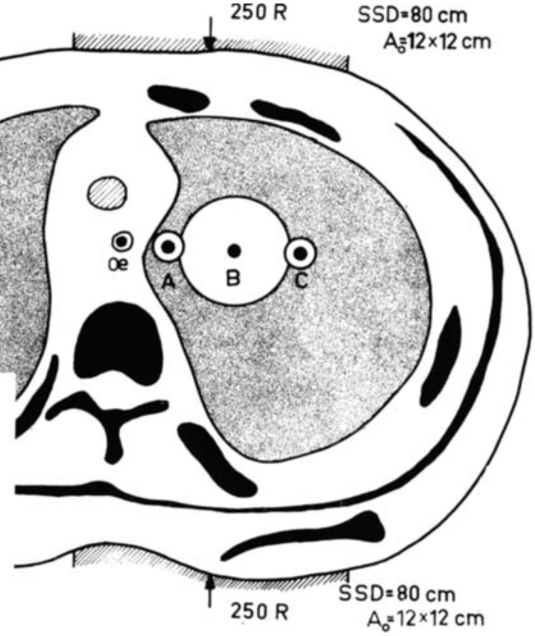

Point	DOSE Calc.	Meas.
Oe	258	261
A	286	269
B	310	296
C	314	302

Fig. 11. Cross-section through an anatomical thorax phantom containing a mix-D cylinder (5 cm in diameter). The positions of the beams are shown. The doses at points A, B, and C and in the oesophagus (Oe) were calculated with the aid of exit dose measurements and measured directly. Dose in rad.

was placed in the lung volume. Two different experimental arrangements were used as shown in Figs 10 and 11. The cross-sections in the figures are representative for the whole volume struck by the beams. The measurements were made with Bg-chambers.

Irradiation with two opposed beams gave the values shown in the figures. The quotients of the measured values and values calculated from exit dose measurements at the relevant points are between 94 % and 102 %. With no correction of the standard isodose charts, quotients of between 99 % and 121 % were obtained.

Discussion

It is essential that regard should be paid to the material beside and behind the measuring chamber, if the exit dose is to be used clinically for the calculation of the dose distribution. The formulas which have been derived above are valid, within the given margins of error, only if the scattered radiation corresponds to that existing in a large phantom. When a patient is exposed to radiation some material must either be placed behind and beside the exit-dose measuring-chamber so as to provide this scattered radiation, or a correction must be made for the reduced scatter. The order of magnitude of this correction, when measuring with Bg-chambers, was investigated. The beam was directed at right angles to sheets of mix-D with thicknesses of 10, 20 and 30 cm, respectively, in three different measuring arrangements. A 0.5 cm thick perspex sheet was placed behind mix-D, the Bg-chambers lying in this perspex sheet. Irradiations were made with field sizes of 7.5 × 7.5 cm and 15 × 15 cm (SSD 80 cm), with air and mix-D, respectively, behind the chambers. This resulted in a voltage drop between 95 % and 90 % with air as compared with mix-D placed behind the chambers for the same dose at a depth of 0.5 cm within the phantom.

For irradiation of the thorax in individual patients, calculation of the dose distribution is difficult. This is largely due to the problem of establishing the variations in density in the volume to be irradiated. An accurate correction will depend upon the dimensions of the lungs and on knowledge of how radiation is absorbed and scattered in the various parts of the lungs.

With three-dimensional dose calculations based on exit dose measurements, the degree of accuracy stated above is obtained without these relationships being known. This method has the additional advantage that correction for bone tissue, for oblique incidence and for different beam sizes may be made at the same time. When calculating the dose in the central plane, the accuracy is independent of error in measurements of the patient thickness.

SUMMARY

A method of calculating the dose in three dimensions in a patient with the aid of exit dose measurements is described and discussed. Particular attention is paid to the conditions when the beam strikes the body obliquely and when it passes through an air-filled lung, the deviation between the measured and calculated doses being within ± 3 % and ± 10 %, respectively.

ZUSAMMENFASSUNG

Eine Methode zur Bestimmung der Dosisverteilung in drei Dimensionen mit Hilfe der Messung der Austrittsdosis wird beschrieben und erörtert. Besondere Aufmerksamkeit wird den Bedingungen gewidmet, wenn dass Strahlenbündel schräg den Körper trifft und wenn es durch eine luftgefüllte Lunge passiert. Die Abweichung zwischen den gemessenen und errechneten Werten liegt innerhalb ± 3 % beziehungsweise innerhalb ± 10 %.

RÉSUMÉ

L'auteur décrit et étudie une méthode de calcul de la dose dans les trois dimensions sur un malade, à partir des mesures des doses de sortie. Il a étudié particulièrement les cas où le rayonnement tombe à l'oblique sur le corps et où il traverse le poumon rempli d'air. L'écart entre la dose mesurée et la dose calculée était de $\pm$ 3 % dans le premier cas, et $\pm$ 10 % dans le second cas.

REFERENCES

Benner S., Ragnhult I., and Gebert G.: Miniature ionization chambers for measurements in body cavities. Phys. in Med. Biol. 4 (1959), 26.

Burlin T. E.: The evaluation of the dose to the thorax in rotational cobalt 60 therapy. Brit. J. Radiol. 30 (1957), 543.

Dahl O., and Vikterlöf K. J.: Attainment and value of precision in deep radiotherapy. Acta radiol. (1960) Suppl. 189.

Depth dose tables for use in radiotherapy. Brit. J. Radiol. (1961) Suppl. 10.

Du Sault L. A., and Legaré J.-M.: Dosage calculations for oblique beams of radiation. Radiology 80 (1963), 856.

Dutreix A., and Dutreix J.: Construction des isodoses pour les surfaces obliques et irrégulières. J. Radiol. Eléctrol. 43 (1962), 671.

Garrett J. H., and Jones D. E. A.: Dose distribution problems in megavoltage therapy. II. Obliquity problems in megavoltage therapy. Brit. J. Radiol. 35 (1962), 739.

Hultberg S., Dahl O., Thoraeus R., Vikterlöf K. J., and Walstam R.: Kilocurie cobalt 60 therapy at the Radiumhemmet. Acta radiol. (1959) Suppl. 179.

— — — — — The 4 000 curie cobalt 60 therapy installation at Radiumhemmet. Acta radiol. 58 (1962), 1.

ICRU Report 10d. NBS Handbook 87, Washington 1963.

Johns H. E.: The physics of radiology. Second edition, Chapter XI. Charles C. Thomas, Springfield, Illinois 1961.

Kornelsen R. O.: Tumour dose in the chest cavity. Brit. J. Radiol. 27 (1954), 289.

Larsson I., Lidén K., and Starfelt M.: Automatic isodose recorder. Acta radiol. Ther. Phys. Biol. 1 (1963), 29.

Sievert R. M.: Über die Anwendung der Kondensatorkammer für sowohl Röntgen- wie γ-Strahlen-Messungen; zugleich ein Beitrag zu den Vorgleichen der biologischen Wirkungen dieser beiden Strahlenarten. Acta radiol. 15 (1934), 193.

Sköldborn H.: On the design, physical properties and practical application of small condenser ionisation chambers. Acta radiol. (1959) Suppl. 187.

Sundbom L.: Individually designed filters in cobalt 60 teletherapy. Acta radiol. Ther. Phys. Biol. 2 (1964), 189.

Woodley R. G., Bronstein E. L., and Laughlin J. S.: Exit dosimeter for effective patient thickness. Radiology 74 (1960), 273.